Quantum Bubbles in Microgravity

A. Tononi[1,*] F. Cinti[2,3,4,†] and L. Salasnich[1,5,‡]

[1]*Dipartimento di Fisica e Astronomia "Galileo Galilei," Università di Padova, via Marzolo 8, Padova 35131, Italy*
[2]*Dipartimento di Fisica e Astronomia, Università di Firenze, I-50019 Sesto Fiorentino (FI), Italy*
[3]*INFN, Sezione di Firenze, I-50019 Sesto Fiorentino (FI), Italy*
[4]*Department of Physics, University of Johannesburg, P.O. Box 524, Auckland Park 2006, South Africa*
[5]*Istituto Nazionale di Ottica (INO) del Consiglio Nazionale delle Ricerche (CNR),
via Nello Carrara 1, Sesto Fiorentino 50125, Italy*

The recent developments of microgravity experiments with ultracold atoms have produced a relevant boost in the study of shell-shaped ellipsoidal Bose-Einstein condensates. For realistic bubble-trap parameters, here we calculate the critical temperature of Bose-Einstein condensation, which, if compared to the one of the bare harmonic trap with the same frequencies, shows a strong reduction. We simulate the zero-temperature density distribution with the Gross-Pitaevskii equation, and we study the free expansion of the hollow condensate. While part of the atoms expands in the outward direction, the condensate self-interferes inside the bubble trap, filling the hole in experimentally observable times. For a mesoscopic number of particles in a strongly interacting regime, for which more refined approaches are needed, we employ quantum Monte Carlo simulations, proving that the nontrivial topology of a thin shell allows superfluidity. Our work constitutes a reliable benchmark for the forthcoming scientific investigations with bubble traps.

The recent advances in microgravity experiments with Bose-Einstein condensates have recently allowed us to extend the intrinsic limits of ground-based experiments and to realize exotic confining potentials for systems of ultracold atoms [1–6]. In particular, the seminal proposal by Zobay and Garraway to produce matter-wave condensate bubbles [7–9] is currently under investigation in NASA cold atom laboratory (CAL) on the international space station [10]. Experimentally, shell-shaped atomic traps are engineered by an adiabatic deformation of a conventional magnetic trap with a radio frequency field. A quasi-two-dimensional hollow condensate can however be obtained only in microgravity conditions, since without any mechanism to compensate for gravity the atoms fall to the bottom of the trap [11–13].

Spherically symmetric hollow condensates have a rich low-energy dynamical behavior [14–17], and the interplay of curvature, nontrivial contact interaction [18], and finite-size give rise to an interesting phase diagram in the thin-shell limit [19–21]. Moreover, it is expected that dipolar interactions induce anisotropic density profiles [22,23], while for soft-core interactions a clusterization phenomenon is suggested [24]. In other hollow configurations as ring and toroidal traps [25] a cooling quench may induce superfluid currents via the Kibble-Zurek mechanism [26–28], but the adiabaticity requirements for bubble traps should prevent this phenomenon. All the recent papers deal with the simplified geometry of a spherical shell, and a complete physical description of the quantum statistics of an ellipsoidal shell is currently lacking.

Inspired by the planned microgravity experiments [10], we investigate the physics of a bosonic system of particles confined on an ellipsoidal shell. We calculate the critical temperature for Bose-Einstein condensation T_{BEC} with a self-consistent Hartree-Fock (HF) theory [29,30]. We find that, when the atoms are adiabatically transferred from the bare harmonic trap to the bubble trap, T_{BEC} decreases up to a factor of 10. This is partly due to the trap geometry, and partly due to a reduced maximal local density, which we estimate at T_{BEC} with the HF theory, and at $T = 0$ with the Gross-Pitaevskii equation [31,32]. We also simulate the free expansion of the ellipsoidal shell: the peculiar topology of our system results in a new interference pattern, with qualitative differences from that of the harmonically trapped condensate. For temperatures lower than 5 nK, mainly for $N \lesssim 5 \times 10^3$ particles, our semiclassical approach breaks down. To investigate quantitatively the coherence properties in this regime, we adopt a first-principle path integral Monte Carlo (PIMC) numerical approach [33], which can accurately predict the physics of a mesoscopic trapped system [34].

Our results are of great relevance for the forthcoming experiments with bubble traps, and for the future developments of microgravity physics, allowing a greater understanding of Bose-Einstein condensation and superfluidity in curved and compact manifolds.

We consider a system of ^{87}Rb atoms in the hyperfine state $|F = 2, m_F = 2\rangle$, confined in the three-dimensional harmonic potential $u(\vec{r}) = m(\omega_x^2 x^2 + \omega_y^2 y^2 + \omega_z^2 z^2)/2$, where m is the atomic mass, $\vec{\omega} = (\omega_x, \omega_y, \omega_z)$ are frequencies of the confinement, and $\vec{r} = (x, y, z)$. A shell-shaped condensate can be obtained by tuning a radio frequency magnetic field with a detuning Δ, which must be much larger than the Rabi frequency Ω between the hyperfine levels [10]. If this dressing procedure is performed adiabatically, and under the hypothesis that any gravitational effect can be neglected [35], the atoms will be confined by the bubble-trap potential [7]

$$U(\vec{r}) = M_F \sqrt{[u(\vec{r})/2 - \hbar\Delta]^2 + (\hbar\Omega)^2}, \qquad (1)$$

where $M_F = 2$ now labels the higher dressed state with energy $U(\vec{r})$, and $\hbar$ is the Planck constant.

Adopting Eq. (1) for the realistic experimental parameters of Ref. [10], here we calculate the critical temperature T_{BEC} of the transition between a noncondensed cloud and a Bose-Einstein condensate. With a self-consistent Hartree-Fock theory [29], the sum over all occupation numbers of thermal states, given by the Bose distribution at a fixed critical temperature T_{BEC}, is equal to the critical number of atoms N at that temperature. In particular, the quasiparticle excitation spectrum appearing in the Bose distribution is treated semiclassically as $E(\vec{p}, \vec{r}) = p^2/2m + U(\vec{r}) + 2g_0 n(\vec{r})$, where $n(\vec{r})$ is the number density, p is the momentum of the excitation, $g_0 = 4\pi\hbar^2 a_s/m$ is the zero-range interaction strength, and $a_s = a_{Rb}$ is the three-dimensional s-wave scattering length of ^{87}Rb. The external potential $U(\vec{r})$ is given by Eq. (1), in which we choose $\vec{\omega}/(2\pi) = (30, 100, 100)$ Hz, and set $\Omega/(2\pi) = 5$ kHz [10] throughout the Letter. Different trapping configurations, from thicker shells with a small size, to thinner ones with a larger size, can be obtained by choosing increasing values of the detunings Δ, which can be experimentally tuned to engineer different traps.

Our results are summarized in Fig. 1, in which T_{BEC} is reported as a function of the particle number N (top panel), and of the detuning Δ (bottom panel). The top panel clearly shows that quantum degeneracy is harder to reach in bubble traps than in conventional harmonic traps, with the critical temperature decreasing up to a factor of 10. Thus, even if the atomic cloud cools during the adiabatic deformation of the trap [36], when the temperature in the predressed harmonic potential is not low enough an initial condensate may become a thermal cloud. We emphasize that, for a fixed particle number, the critical temperature of a thinner shell [$\Delta/(2\pi) = 30$ kHz, green thick line] is slightly lower than the one of a thicker shell [$\Delta/(2\pi) = 10$ kHz, grey dashed line]. A complementary picture is given by the bottom panel of Fig. 1, where the critical temperature is shown to decrease quickly for an increasing detuning, with $\Delta = 0$ corresponding to the bare harmonic trap (see also
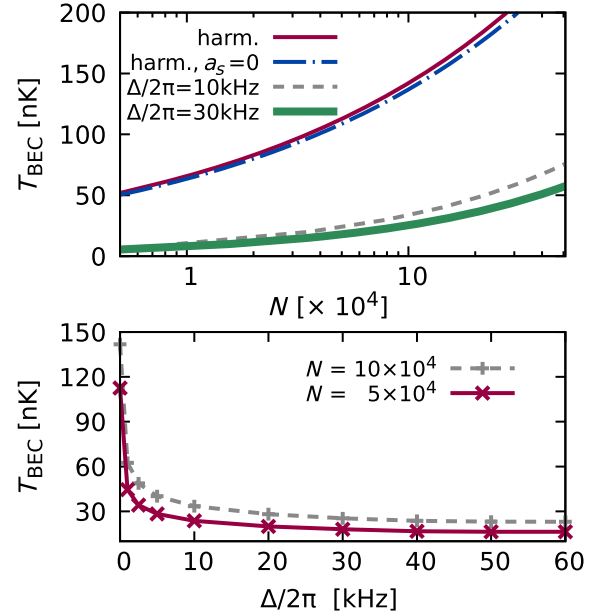

FIG. 1. Critical temperature for Bose-Einstein condensation T_{BEC} as a function of the number of particles N (top) and detuning Δ (bottom). Top: comparison for different external potentials: harmonic trap with $\vec{\omega}/(2\pi) = (30, 100, 100)$ Hz (red thin line), noninteracting bosons in a harmonic trap [40] (blue dot-dashed line), bubble trap with $\Delta/(2\pi) = 10$ kHz (grey dashed line), bubble trap with $\Delta/(2\pi) = 30$ kHz (green thick line). Bottom: as soon as Δ is nonzero T_{BEC} decreases partly due to the reduced maximal local density, becoming essentially constant for large detunings [37].

Ref. [37]). Further simulations show that, tuning the s-wave scattering length up to a factor 5 of the bare value for ^{87}Rb, the critical number of particles decreases up to 20% of Fig. 1 values. Moreover, we verified that this approach reproduces our previous results for a thin spherical shell [19] as long as $N \gtrsim 10^5$ and $\Delta \gg \Omega \gg \omega$.

With respect to current experiments, the previous results neglect the inhomogeneities of the potentials, which can be quantified as a $0.001g$ tilt of the trap [10], with g the acceleration of gravity at the Earth level. Under this hypothesis, we can also safely neglect the residual micro-gravitational corrections ($\sim 10^{-6}g$) [10]. While the inhomogeneities affect the atomic spatial distribution [10], preventing a uniform condensation along the shell, we find that the critical temperatures of Fig. 1 are practically unchanged.

The validity of our HF theory relies on the inequality $k_B T > \hbar\omega_0$, where ω_0 is the typical frequency spacing between the levels of the system [29]. Following Ref. [16], we estimate $\omega_0 = \bar{\omega}\sqrt{2\Delta/\Omega}$, with $\bar{\omega} = (\omega_x\omega_y\omega_z)^{1/3}$ the geometric average of the harmonic trap frequencies, so that the minimum temperatures at which the semiclassical approximation is expected to hold are $\hbar\omega_0/k_B \approx 5$ nK. Our theory is reliable over this critical temperature, which corresponds to $N \gtrsim 5 \times 10^3$.

For a fixed particle number N, at temperatures sufficiently lower than those identified in Fig. 1, all the particles of this weakly interacting system can be approximately thought to be in the same single-particle state. In this zero-temperature fully condensate regime, the macroscopic wave function of the system $\psi(\vec{r}, t)$ satisfies the Gross-Pitaevski equation (GPE) [31,32]

$$i\hbar \frac{\partial \psi(\vec{r}, t)}{\partial t} = \left[-\frac{\hbar^2 \nabla^2}{2m} + U(\vec{r}) + g_0 |\psi(\vec{r}, t)|^2 \right] \psi(\vec{r}, t). \tag{2}$$

The stationary solution of Eq. (2) gives the condensate density at zero temperature, i.e., $n(\vec{r}) = |\psi(\vec{r})|^2$. In particular, by using an imaginary-time propagation algorithm [41], here we solve the GPE for $N = 57100$ bosons trapped in the external potential of Eq. (1) with $\Delta/(2\pi) = 30$ kHz, and $\Omega/(2\pi) = 5$ kHz [42]. In the top panel of Fig. 2 we plot a two-dimensional section of the condensate density $n(\vec{r})$, cut along the xz plane. For simplicity, we avoid showing the density distribution along the xz plane, due to the trivial axial symmetry of the confinement. We find that the particles are not uniformly distributed on the shell, but accumulate on the ellipsoid lobes, where the local ellipsoidal trapping is weaker. This nonuniform particle distribution across the shell can be also seen in the bottom panels of Fig. 2, in which we plot the one-dimensional cuts
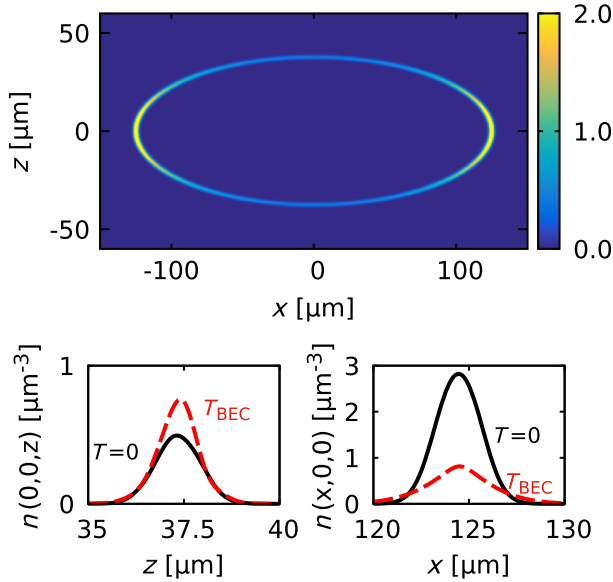
of the condensate density $n(\vec{r})$ along the x and the z direction ($T = 0$ label) [43]. It is quite interesting to compare the condensate distribution with the thermal density at the critical temperature T_{BEC}, obtained from the HF theory (T_{BEC} label). Similarly to harmonically trapped gases [29], while the condensate density at $T = 0$ is more localized in the vertices, the thermal cloud is broader and practically uniform: this crucial difference can be used as a first experimental check of the temperature of the system. At the same time, given the current status of microgravity experiments, the observation of these effects requires a precise control of the inhomogeneities of the radio frequency field, to get a full and symmetric coverage of the shell. This is the object of ongoing experimental efforts on CAL [10], towards the next generation of experiments on BECCAL [2].

To analyze more deeply the physics of bubble-trapped condensates we now study the dynamics of the system, by solving numerically Eq. (2) [44]. The peculiar signatures of a hollow Bose-Einstein condensate clearly emerge in the free expansion of the system. In this case, without any magnetic confinement, the hyperfine splitting of the atomic energy levels is absent, and the simulation of a single GPE is sufficient [45]. Starting from the stationary solution of Eq. (2) for $\Delta/(2\pi) = 10$ kHz and $N = 57100$ bosons, we suddenly remove the trapping potential $U(\vec{r})$ at the time $t = 0$ ms. During the dynamics of the system we take three snapshots of the density in the xz plane, for 4.5, 9, and 18 ms. The last panel of Fig. 3 depicts the interesting interference pattern obtained when the matter-wave self interferes at the center of the trap. As a qualitative difference with respect to harmonically trapped condensates

FIG. 2. Top: contour plot of the density in the xz plane (colorbox units in μm^{-3}), obtained solving Eq. (2), for $\vec{\omega}/(2\pi) = (30, 100, 100)$ Hz, $\Delta/(2\pi) = 30$ kHz, $\Omega/(2\pi) = 5$ kHz, and $N = 57100$. Bottom: one-dimensional sections of the density at $T = 0$ (from the GPE) and at T_{BEC} (from Hartree-Fock theory). Note that at $T = 0$ the condensate is concentrated on the shell vertices, while the thermal cloud at T_{BEC} is uniformly distributed.
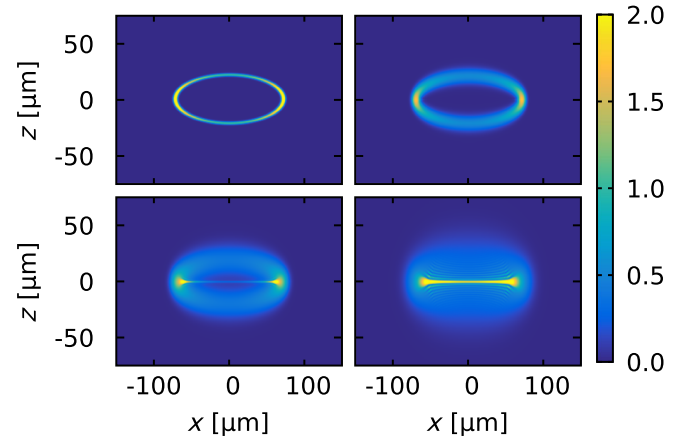

FIG. 3. Free expansion of the condensate shell, initially in the ground state for the bubble-trap potential of Eq. (1) with $\Delta/(2\pi) = 10$ kHz, and the other parameters as in Fig. 2. From left to right and from top to bottom, the condensate slices along the xz plane are taken at the times: 0 ms, 4.5 ms, 9 ms, and 18 ms. The hollow condensate expands both outwards and inwards, showing a qualitatively different interference pattern with respect to that of harmonic traps [37,46].

[37], here we observe the appearance of a central density peak around the final time of 18 ms. Since the free expansion of the condensate cloud takes place in a ~ 10 ms time, and the main interference peak has a width of approximately 4 μm [37], this phenomenon is easily observable in current microgravity experiments.

For a low number of particles, the Hartree-Fock theory is not expected to describe accurately the physics of the system. In this regime, we describe the coherence properties through a continuous-space worm algorithm PIMC numerical simulation [47,48]. This technique allows us to simulate the exact dynamics of the system, described by the general Hamiltonian

$$\mathcal{H} = -\frac{1}{2}\sum_{i=1}^{N}\nabla^2 + \sum_{i=1}^{N} U(\vec{r}_i) + \sum_{i<j}^{N} v(|\vec{r}_i - \vec{r}_j|), \quad (3)$$

in which the particles are interacting with the hardcore potential $v(|\vec{r}_i - \vec{r}_j|) = \infty$ for $|\vec{r}_i - \vec{r}_j| < r_0$, with r_0 the hardcore potential range, and 0 otherwise. We stress that in the Hamiltonian (3) we have rescaled all the energies with $\hbar^2/(mr_0^2)$, the typical energy of the two-body interaction. In particular, for our interaction potential the range r_0 can be identified with the three-dimensional s-wave scattering length a_s [49].

In order to observe superfluidity in dilute systems of few particles ($N \lesssim 10^3$), it is crucial that the interaction between bosons is strong enough. In this case, the critical rotational frequency of the trap $\Omega_c \approx g_0 n/\hbar$ under which superfluidity can occur will be sufficiently large, and the system will be in the Thomas-Fermi regime. Clearly, the experimental observation of superfluidity in a mesoscopic system is a trade-off between the necessity of having a long enough lifetime of the condensate to perform measures, and the intrinsic limits of the cooling apparatus. To discuss temperature regimes that are relevant for the current experimental capabilities ($T \gtrsim$ nK), we model a Bose gas in which the scattering length is tuned with a Feshbach resonance to the value $a_s = ca_{\mathrm{Rb}}$, where a_{Rb} is the bare scattering length of ^{87}Rb [50]. The scattering length of ^{87}Rb can be tuned with the 1007G Feshbach resonance [51,52] up to $c \approx 10$, at least without reducing significantly the number of trapped atoms. For a mesoscopic system, we suggest that c can reasonably be tuned up to $25 \div 50$.

The results of our simulations are shown in Fig. 4. In particular, Fig. 4(a) depicts an instantaneous configuration of $N = 512$ bosons at a temperature of $T = 4.4$ nK, featuring the projection of world lines onto real space. These projections have the important insight to be the closest representation of the square of the many-body wave function [33,53]. As a result, Fig. 4(a) displays an evident paths overlapping which implies exchanges among delocalized particles and hence global superfluidity. This claim finds agreement with Fig. 4(b) where we report the relative probability $P(n)$ that n-particles exchange within the
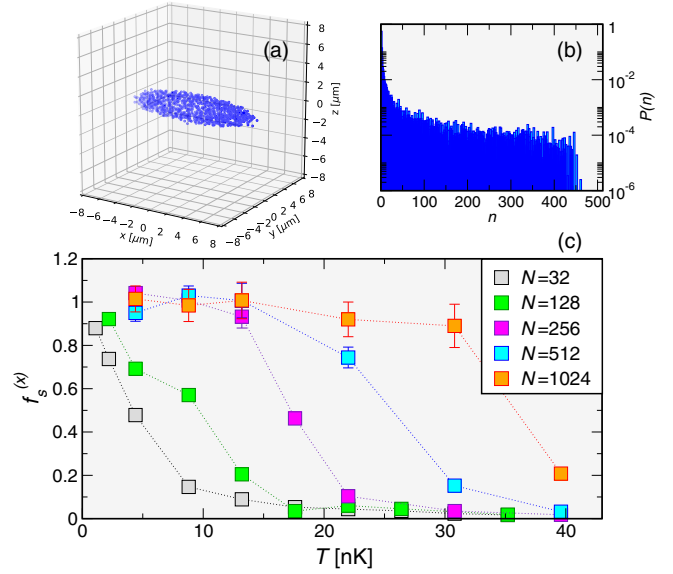

FIG. 4. Results of the Monte Carlo simulations, in which we employ the bubble-trap potential of Eq. (1) with $\vec{\omega}/(2\pi) = (0.2, 1, 1)$ kHz, $\Delta/(2\pi) = 10$ kHz, $\Omega/(2\pi) = 5$ kHz, and $a_s = 50a_{\mathrm{Rb}}$. In (a) we represent the real space projection of the wordlines for $N = 512$ bosons at 4.4 nK. The superfluid character of this configuration is proven in panel (b), by the fat-tailed distribution $P(n)$ of the n-particles permutation cycles, with $1 \leq n \leq N$. We summarize our simulations in panel (c), showing the superfluid fraction of the system $f_s^{(x)}$ as a function of the temperature T.

bubble-trap confinement $U(\vec{r})$. Note that $P(n)$ is nonzero on an extended region of n, concerning long permutation cycles (exchanges) of the order of $n \lesssim N$.

Let us now quantitatively discuss the phenomenon of superfluidity in this strongly interacting hollow gas. In a confined system, the superfluid fraction can be calculated as the ratio of the nonclassical inertial moment I_i and the classical one I_i^{cl}, the index i being one of the main axes along the directions x, y, and z. Thus, the estimator of the superfluid fraction $f_s^{(i)}$ is given by [54–56] $f_s^{(i)} = 4m^2\langle A_i^2\rangle/(\hbar^2\beta\langle I_i^{\mathrm{cl}}\rangle)$, where $\beta = 1/k_BT$, while $\langle\cdots\rangle$ stands for the thermal average, and A_i underlies the world-line area of closed particle trajectories projected on its corresponding perpendicular plane [54–56]. The superfluid fraction $f_s^{(x)}$ is reported in Fig. 4(c) as a function of the temperature T, showing the results of the sampling for N ranging from 32 to 1024 bosons. We stress that, when increasing the number of bosons N, the coherence effects are enhanced, and a sizeable superfluid fraction is reached at higher temperatures. Regarding $f_s^{(y)}$ and $f_s^{(z)}$, we find that they result systematically lower than $f_s^{(x)}$ by a factor of 5 [37]. This result implies an anisotropic second sound velocity, which in a two-dimensional weakly interacting bosonic system goes as $c_2^{(i)} \propto (f_s^{(i)})^{1/2}$ [57]. Experimentally, a density perturbation in a sufficiently

large and flat shell will then show that $c_2^{(x)} > c_2^{(z)}$ [37]. Similarly to what we have deduced with the HF theory, we have verified that for fixed N and a_s, the superfluid fraction is lower for thinner and larger ellipsoidal shells, in which the collective behavior is suppressed. Moreover, we have also verified that the typical temperature range at which $f_s^{(x)}$ becomes significant in a bubble-trap are up to a factor of 5 lower than the ones for a harmonically trapped gas. Finally, since we are simulating a finite-size small system, there is not a finite temperature at which the superfluid fraction vanishes, but increasing N the transition will get sharper and the residual $f_s^{(x)}$ will tend to zero. All these observations clearly show that, despite the topology of a thin shell-shaped condensate is different from the one of the 2D flat plane, the system is superfluid.

To conclude, we have calculated the critical temperature for Bose-Einstein condensation of a bosonic system of atoms confined on a shell-shaped potential, finding that, with respect to the bare harmonic trap, the critical temperature is significantly lower. We have then simulated the Gross-Pitaevskii equation with the realistic external potential parameters to describe the ground state and the free expansion of the system, observing an interesting self-interference pattern during the hole filling. Finally, we have shown that for a mesoscopic number of particles in a regime of strong interactions the thin atomic shell is superfluid for experimentally accessible temperature regimes. Our findings will be of great interest for modeling and understanding the ongoing experiments with microgravity Bose-Einstein condensates.

[*]Corresponding author.
andrea.tononi@phd.unipd.it
[†]fabio.cinti@unifi.it
[‡]luca.salasnich@unipd.it

[1] E. R. Elliott, M. C. Krutzik, J. R. Williams, R. J. Thompson, and D. C. Aveline, npj Microgravity **4**, 16 (2018).
[2] K. Frye *et al.*, arXiv:1912.04849.
[3] T. van Zoest *et al.*, Science **328**, 1540 (2010).
[4] M. Meister, A. Roura, E. M. Rasel, and W. P. Schleich, New J. Phys. **21**, 013039 (2019).
[5] D. Becker, K. Frye, C. Schubert, and E. M. Rasel, Bull. Am. Phys. Soc. **63** (2018).
[6] D. C. Aveline, J. R. Williams, E. R. Elliott *et al.*, Nature (London) **582**, 193 (2020).
[7] O. Zobay and B. M. Garraway, Phys. Rev. Lett. **86**, 1195 (2001).
[8] O. Zobay and B. M. Garraway, Phys. Rev. A **69**, 023605 (2004).
[9] B. M. Garraway and H. Perrin, J. Phys. B **49**, 172001 (2016).
[10] N. Lundblad, R. A. Carollo, C. Lannert, M. J. Gold, X. Jiang, D. Paseltiner, N. Sergay, and D. C. Aveline, npj Microgravity **5**, 30 (2019).
[11] Y. Colombe, E. Knyazchyan, O. Morizot, B. Mercier, V. Lorent, and H. Perrin, Europhys Lett. **67**, 593 (2004).
[12] M. White, H. Gao, M. Pasienski, and B. DeMarco, Phys. Rev. A **74**, 023616 (2006).
[13] T. L. Harte, E. Bentine, K. Luksch, A. J. Barker, D. Trypogeorgos, B. Yuen, and C. J. Foot, Phys. Rev. A **97**, 013616 (2018).
[14] C. Lannert, T.-C. Wei, and S. Vishveshwara, Phys. Rev. A **75**, 013611 (2007).
[15] K. Padavic, K. Sun, C. Lannert, and S. Vishveshwara, Europhys. Lett. **120**, 20004 (2018).
[16] K. Sun, K. Padavic, F. Yang, S. Vishveshwara, and C. Lannert, Phys. Rev. A **98**, 013609 (2018).
[17] N. S. Móller, F. E. A. dos Santos, V. S. Bagnato, and A. Pelster, arXiv:2001.07443.
[18] J. Zhang and Tin-Lun Ho, J. Phys. B **51**, 115301 (2018).
[19] A. Tononi and L. Salasnich, Phys. Rev. Lett. **123**, 160403 (2019).
[20] B. A. Ovrut and S. Thomas, Phys. Rev. D **43**, 1314 (1991).
[21] S. J. Bereta, L. Madeira, M. A. Caracanhas, and V. S. Bagnato, Am. J. Phys. **87**, 924 (2019).
[22] S. K. Adhikari, Phys. Rev. A **85**, 053631 (2012).
[23] P. C. Diniz, E. A. B. Oliveira, A. R. P. Lima, and E. A. L. Henn, Sci. Rep. **10**, 4831 (2020).
[24] S. Prestipino and P. V. Giaquinta, Phys. Rev. A **99**, 063619 (2019).
[25] C. Ryu, M. F. Andersen, P. Cladé, V. Natarajan, K. Helmerson, and W. D. Phillips, Phys. Rev. Lett. **99**, 260401 (2007).
[26] T. W. B. Kibble, J. Phys. A **9**, 1387 (1976).
[27] W. H. Zurek, Nature (London) **317**, 505 (1985).
[28] L. Corman, L. Chomaz, T. Bienaimé, R. Desbuquois, C. Weitenberg, S. Nascimbène, J. Dalibard, and J. Beugnon, Phys. Rev. Lett. **113**, 135302 (2014).
[29] S. Giorgini, L. P. Pitaevskii, and S. Stringari, J. Low Temp. Phys. **109**, 309 (1997).
[30] L. Pitaevski and S. Stringari, *Bose-Einstein Condensation and Superfluidity* (Oxford University Press, Oxford, 2016).
[31] E. P. Gross, Nuovo Cimento (1955–1965) **20**, 454 (1961).
[32] L. P. Pitaevskii, Sov. Phys. JETP **13**, 451 (1961).
[33] D. M. Ceperley, Rev. Mod. Phys. **67**, 279 (1995).
[34] N. Henkel, F. Cinti, P. Jain, G. Pupillo, and T. Pohl, Phys. Rev. Lett. **108**, 265301 (2012).
[35] Performing the experiments in microgravity allows us to neglect the additional mgz contribution to the external potential, which affects ground-based experiments [11].
[36] N. Lundblad (private communication).

[37] See the Supplemental Material at http://link.aps.org/supplemental/10.1103/PhysRevLett.125.010402 for additional details on Fig. 1, on the free expansion, and on the PIMC results, which includes Refs. [38,39].

[38] J. L. Ville, R. Saint-Jalm, É. Le Cerf, M. Aidelsburger, S. Nascimbène, J. Dalibard, and J. Beugnon, Phys. Rev. Lett. **121**, 145301 (2018).

[39] A. Cappellaro, F. Toigo, and L. Salasnich, Phys. Rev. A **98**, 043605 (2018).

[40] F. Dalfovo, S. Giorgini, L. P. Pitaevskii, and S. Stringari, Rev. Mod. Phys. **71**, 463 (1999).

[41] M. L. Chiofalo, S. Succi, and M. P. Tosi, Phys. Rev. E **62**, 7438 (2000).

[42] We employ these parameters to be to be as close as possible to the experiments, and to the previous literature on this topic, see Ref. [10].

[43] The level of discretization for this two-dimensional condensate does not allow to observe the radial discontinuities in the density profile of Ref. [29].

[44] W. H. Press et al., Numerical Recipes 3rd Edition: The Art of Scientific Computing (Cambridge University Press, New York, 2007), https://dl.acm.org/doi/10.1145/1874391.187410.

[45] In principle the s-wave scattering length for the atoms in the various hyperfine levels can be different, but due to the low atomic density of approximately 10^{12} cm^{-3} the use of g_0 is a good approximation.

[46] L. Salasnich, N. Manini, F. Bonelli, M. Korbman, and A. Parola, Phys. Rev. A **75**, 043616 (2007).

[47] M. Boninsegni, N. V. Prokofev, and B. V. Svistunov, Phys. Rev. E **74**, 036701 (2006).

[48] M. Boninsegni, N. Prokofev, and B. Svistunov, Phys. Rev. Lett. **96**, 070601 (2006).

[49] H. T. C. Stoof, D. B. M. Dickerscheid, and K. Gubbels, Ultracold Quantum Fields (Springer, Dordrecht, 2009).

[50] M. Egorov, B. Opanchuk, P. Drummond, B. V. Hall, P. Hannaford, and A. I. Sidorov, Phys. Rev. A **87**, 053614 (2013).

[51] A. Marte, T. Volz, J. Schuster, S. Dürr, G. Rempe, E. G. M. van Kempen, and B. J. Verhaar, Phys. Rev. Lett. **89**, 283202 (2002).

[52] G. Smirne, R. M. Godun, D. Cassettari, V. Boyer, C. J. Foot, T. Volz, N. Syassen, S. Dürr, G. Rempe, M. D. Lee, K. Góral, and T. Köhler, Phys. Rev. A **75**, 020702(R) (2007).

[53] F. Cinti, A. Cappellaro, L. Salasnich, and T. Macrì, Phys. Rev. Lett. **119**, 215302 (2017).

[54] Y. Kwon, F. Paesani, and K. B. Whaley, Phys. Rev. B **74**, 174522 (2006).

[55] P. Jain, F. Cinti, and M. Boninsegni, Phys. Rev. B **84**, 014534 (2011).

[56] T. Zeng and P.-N. Roy, Rep. Prog. Phys. **77**, 046601 (2014).

[57] T. Ozawa and S. Stringari, Phys. Rev. Lett. **112**, 025302 (2014).